

# Ultralight micro-perforated sandwich panel with hierarchical honeycomb core for sound absorption

*Journal of Sandwich Structures and Materials*

0(0) 1–17

© The Author(s) 2021

Article reuse guidelines:

[sagepub.com/journals-permissions](https://sagepub.com/journals-permissions)

DOI: 10.1177/1099636221993880

[journals.sagepub.com/home/jsm](https://journals.sagepub.com/home/jsm)

Wei He<sup>1,2,3</sup>, Xiangjun Peng<sup>1,2,3</sup>,  
Fengxian Xin<sup>1,3</sup>  and Tian Jian Lu<sup>2,3,4</sup>

## Abstract

A theoretical model is developed to study the superior sound absorption performance of ultralight micro-perforated sandwich panels with double-layer hierarchical honeycomb core. Numerical simulations are performed to validate theoretical model predictions and explore physical mechanisms underlying the sound absorption. Systematic parametric study is implemented to investigate the influence of specific structural parameters on sound absorption. To maximize sound absorption, optimal structural parameters of the hierarchical sandwich are obtained using the method of simulated annealing. It is demonstrated that viscous dissipation of the air inside micro-perforations and around inlet/outlet regions dominates sound absorption. Compared to micro-perforated sandwich panels with regular honeycomb core, not only the

<sup>1</sup>State Key Laboratory for Strength and Vibration of Mechanical Structures, Xi'an Jiaotong University, Xi'an, P.R. China

<sup>2</sup>State Key Laboratory of Mechanics and Control of Mechanical Structures, Nanjing University of Aeronautics and Astronautics, Nanjing, P.R. China

<sup>3</sup>MOE Key Laboratory for Multifunctional Materials and Structures, Xi'an Jiaotong University, Xi'an, P.R. China

<sup>4</sup>MIIT Key Laboratory of Multi-functional Lightweight Materials and Structures, Nanjing University of Aeronautics and Astronautics, Nanjing, P. R. China

## Corresponding authors:

Fengxian Xin, MOE Key Laboratory for Multifunctional Materials and Structures, Xi'an Jiaotong University, Xi'an 710049, P.R. China.

Email: [fengxian.xin@gmail.com](mailto:fengxian.xin@gmail.com)

Tian Jian Lu, State Key Laboratory of Mechanics and Control of Mechanical Structures, Nanjing University of Aeronautics and Astronautics, Nanjing 210016, P.R. China.

Email: [tjlu@nuaa.edu.cn](mailto:tjlu@nuaa.edu.cn)

proposed hierarchical construction has much improved load-bearing capacity, but also significantly enhanced sound absorption covers a wide range of frequency.

### **Keywords**

Sound absorption, micro-perforated sandwich panel, hierarchical honeycomb core, structural optimization

## **Introduction**

Hierarchical structures across several length scales are not only common in nature but also widely applied in engineering, such as nacre shell, gecko feet, spider silk, tendon, muscle, bone, wood, polymer, and Eiffel tower [1,2]. The macroscopic property of such a structure is determined by its hierarchical organization and constituent materials, and hence it is feasible to tailor specific hierarchical structure according to actual needs. For example, nacre shell is a crossed lamellar micro-architecture comprised of brick-like aragonite tablets and mortar-like biopolymer interface. After subjected to external loading, tablets slide relative to each other and the surface waviness of tablets makes the structure expand transversely, leading to interfacial strain hardening [3]. That is why the nacre shell possesses extremely higher fracture toughness than its main constituent (aragonite) without sacrificing strength simultaneously [4].

Inspired by the wonder achieved by nacre shell, a hierarchical honeycomb generated by replacing each vertex of a regular hexagonal honeycomb with a smaller similar hexagon was proposed [5]. Repeated substitution of lower-level hierarchical honeycomb nodes for smaller similar hexagons yields higher-order hierarchical honeycomb. The in-plane stiffness of the first and second order hierarchical honeycombs is enhanced up to 2.0 and 3.5 times higher than that of a regular honeycomb having the same mass, respectively. Moreover, it has been demonstrated that element buckling induced by uniaxial compressive load may lead to negative Poisson ratio of hierarchical honeycombs [6]. It has been also shown that the in-plane collapse strength of first order hierarchical honeycomb can reach up to about 1.5 times higher than that of the regular honeycomb with the same mass [7,8]. In terms of energy absorption, the out-of-plane crashworthiness of first and second order hierarchical honeycombs is improved separately by 81.3 and 185.7% compared to regular honeycomb with identical mass [9]. In searching for optimal hierarchical configuration, Ryvkin and Shraga revealed that the fracture toughness of second order hierarchical honeycomb increases by 39% relative to that of regular honeycomb [10]. Overall, hierarchical honeycombs exhibit superior load-bearing capabilities than regular honeycombs.

The micro-perforated panel (MPP) has been envisioned as the next generation sound absorbing materials for its durability, design-ability and low manufacturing

cost. Usually, a MPP absorber is constructed of a thin panel perforated with submillimeter holes and backed by an air cavity. As a result, the MPP has low mechanical strength and should not be used for load-bearing. Besides, the half-absorption bandwidth (the frequency range in which the sound absorption coefficient continuously exceeds 0.5) of the MPP is narrow compared with porous sound absorbing materials [11–13]. To improve the sound absorption performance, investigators used several MPP absorbers to form a parallel absorber array [14–17] or divided the air cavity behind the MPP into domains of different depths and shapes [18–21]. These approaches nonetheless inevitably increase the thickness (volume) of the system and lead to no benefit for structural strength.

In many fields such as aeronautic and aerospace engineering, multi-functional structures with simultaneous sound absorption and load-bearing capacity receive increasing attention, subject to further constrains of low volume and light weight. By inserting a honeycomb core into the air cavity behind the MPP, it has been demonstrated that not only the MPP is structurally strengthened but also the sound absorption peak shifts to lower frequency and the half-absorption bandwidth is widened [22–24]. However, the traditional honeycomb, whether hexagonal or square, only divides the air cavity into subunits of the same volume, and the number of sound absorption peaks is much less in the entire frequency range of sound absorption.

In the current study, the sound absorption performance of ultralight perforated sandwich panel with double-layer hierarchical honeycomb core is theoretically and numerically investigated. The hierarchical honeycomb structure provides greater mechanical support than regular honeycomb and divides the air cavity into domains with different volumes without sacrificing volume of the entire structure. The air in each micro-perforation and the air domain immediately behind form different Helmholtz resonators, generating more sound absorption peaks. In general, the pressure level of sound in the environment is low, and the deformation of the structure caused by incident sound can be neglected. So it is reasonable to assume that the structure is rigid and does not consume any energy of incident sound. In addition, the sound is considered as a harmonic plane wave and impinges perpendicularly on the surface of the structure. Based on electroacoustic analogy, the acoustic surface impedance of the structure is first calculated, which is then used to calculate the sound absorption coefficient. Subsequently, the influence of relevant structural parameters on sound absorption is quantified. Finally, to demonstrate the excellent performance of the proposed hierarchical sandwich structure, an optimal configuration for sound absorption in a frequency range of interest is determined using the simulated annealing algorithm.

## Theoretical model

With reference to Figure 1(a), the perforated sandwich panel with height  $h$  consists of three layers of faceplates and double layers of hierarchical honeycomb core. The top and bottom faceplates have the same thickness  $t_1$  and the thickness of the

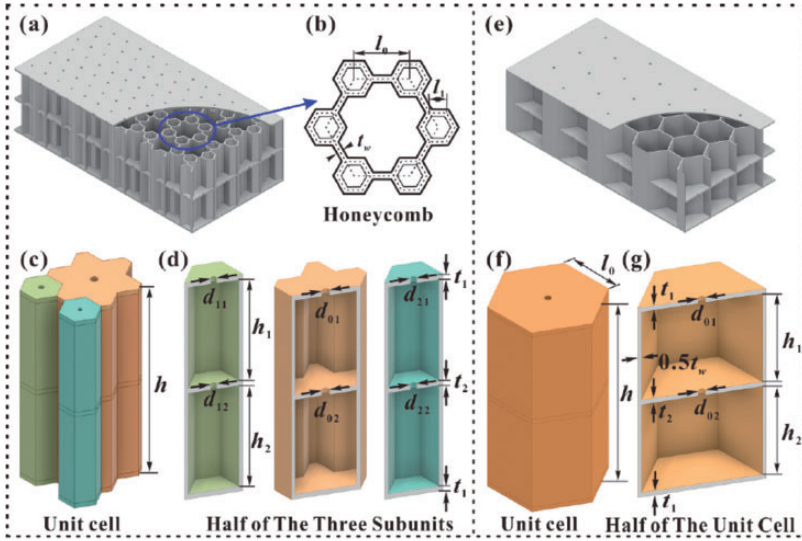


**Figure 1.** Schematic diagram of micro-perforated sandwich panel with: (a) double-layer hierarchical or (e) regular honeycomb core, (b) presents the cross-section of hierarchical honeycomb, (c) and (f) are unit cells of (a) and (b), respectively, (d) and (g) are one-half of (c) and (f), respectively.

middle faceplate is  $t_2$ . The heights of the two honeycomb layers are  $h_1$  and  $h_2$ , respectively. Let  $l_0$  and  $l_1$  denote the edge lengths of the original honeycomb and the introduced smaller honeycomb (Figure 1(b)). The wall thickness of the honeycomb  $t_w$  is uniform everywhere. To avoid the introduced structures overlapping with each other, the ratio of edge lengths  $\gamma = l_1/l_0$  must satisfy:  $0 < \gamma \leq 0.5$ . In the top and middle faceplates, different sub-millimeter-scale circular holes are drilled to connect the inner cavity with external domain. Let  $d_{mn}$  denote the diameter of each micro-perforation, where  $m$  ( $m=0, 1, 2$ ) is the serial number of perforation and  $n$  is used to represent the top faceplate ( $n=1$ ) and the middle faceplate ( $n=2$ ).

The double-layer hierarchical structure of Figure 1(a) is periodic, it suffices to analyze a unit cell as shown in Figure 1(c), which can be further divided into three sub-units (Figure 1(d)). Each sub-unit is composed of two MPPs and two air cavity layers. Because the honeycomb wall occupies a certain space, the effective area of the MPP decreases and is equal to the cross-sectional area of each subunit minus the cross-sectional area of the corresponding honeycomb. That is, it is the same as the cross-sectional area of the sub-cavity.

If the edge lengths of the hierarchical honeycomb,  $l_0$  and  $l_1$ , are much larger than perforation diameters, the mutual interference between the perforations and between the perforation and honeycomb wall can be neglected. Then, the acoustic

surface impedance of a MPP is given by the acoustic impedance of a single tube divided by perforation ratio, as [11,12]

$$Z_{mn}^{MPP} = \frac{j\omega\rho_0 t_n}{p_{mn}} \left[ 1 - \frac{2J_1(x_{mn}\sqrt{-j})}{x_{mn}\sqrt{-j}J_0(x_{mn}\sqrt{-j})} \right]^{-1} + \frac{\sqrt{2}\eta x_{mn}}{p_{mn}d_{mn}} + j\frac{0.85\omega\rho_0 d_{mn}}{p_{mn}} \quad (1)$$

where  $j = \sqrt{-1}$  is the imaginary unit,  $\omega$  is the angular frequency,  $\rho_0 = 1.2 \text{ kg/m}^3$  is the density of air,  $\eta = 1.85 \times 10^{-5} \text{ Pa} \cdot \text{s}$  is the viscosity coefficient of air,  $J_0$  and  $J_1$  are the zeroth and first order Bessel functions of the first kind, respectively, and  $x_{mn} = d_{mn}\sqrt{\rho_0\omega/4\eta}$ . Further,  $p_{mn} = \pi(d_{mn}/2)^2/S_m$  is the perforation ratio, in which  $S_m^{eff}$  is the effective area of the MPP, given by

$$S_m^{eff} = \begin{cases} \sqrt{3}(\sqrt{3}l_0 - t_w)^2/2 - 3\sqrt{3}l_1^2 & (m = 0) \\ \sqrt{3}(\sqrt{3}l_1 - t_w)^2/2 & (m = 1, 2) \end{cases} \quad (2)$$

The last two terms in equation (1) denote end corrections, for the sound radiates at both ends of the perforation and part of the air moves along the MPP panel when it flows in and out of the perforation [25,26]. For the air cavity behind the perforations of each MPP, the acoustic impedance is

$$Z_{mn}^C = \begin{cases} -jZ_0 \cot(\omega h_2/c_0) & (n = 2) \\ Z_0 \frac{(Z_{m2}^{MPP} + Z_{m2}^C)\cos(\omega h_1/c_0) + jZ_0 \sin(\omega h_1/c_0)}{Z_0 \cos(\omega h_1/c_0) + j(Z_{m2}^{MPP} + Z_2^C)\sin(\omega h_1/c_0)} & (n = 1) \end{cases} \quad (3)$$

where  $c_0 = 343 \text{ m/s}$  is the sound speed in air and  $Z_0 = \rho_0 c_0$  is the acoustic impedance of air.

The acoustic surface impedance of each subunit  $Z_m$  is given by

$$Z_m = \delta_m (Z_{m1}^{MPP} + Z_{m1}^C) \quad (4)$$

where  $\delta_m = S_m/S_m^{eff}$  is the correction factor introduced to reflect the influence of honeycomb wall thickness on acoustic surface impedance [27,28], and  $S_m$  is the cross-sectional area of each subunit, given by

$$S_m = \begin{cases} 3\sqrt{3}l_0^2/2 - 3\sqrt{3}l_1^2 & (m = 0) \\ 3\sqrt{3}l_1^2 & (m = 1, 2) \end{cases} \quad (5)$$

According to the parallel-connection rule of acoustical theory, the total acoustic surface impedance of the unit cell  $Z_T$  can be derived from the acoustic surface

impedance of three subunits, as

$$Z_T = \frac{1}{\sum_{m=0}^2 \frac{S_m}{Z_m \times S_T}} \quad (6)$$

where  $S_T = \sum_{m=0}^2 S_m$  is the total cross-sectional area of the unit cell.

The sound absorption coefficient of the sandwich structure is defined as the ratio of absorbed acoustic power to incident acoustic power, given by

$$\alpha = \frac{4\text{Re}(z_s)}{[1 + \text{Re}(z_s)]^2 + [\text{Im}(z_s)]^2} \quad (7)$$

where  $z_s = Z_T/Z_0$  is the relative acoustic surface impedance, and Re and Im represent the real and imaginary parts of a complex, respectively.

## Results and discussion

### Verification of theoretical model

The theoretical analysis detailed in the previous section considers the viscosity of air in and around perforations, but ignores the viscosity of air in the cavities and the thermal conductivity of air in all domains. To fully characterize the sound absorption performance of the proposed sandwich structure, numerical simulations with the commercial finite element (FE) software COMSOL Multiphysics are carried out. Due to rigidity of the structure, only air domains inside and near the structure need to be modelled in FE analysis, as shown in Figure 2. Three cut planes, A, B and C, are used to explore in detailed the physical mechanisms of sound absorption, which are difficult to capture with theoretical modeling. The uppermost air domain, modelled with the Pressure Acoustics module, is used to apply a plane sound wave normally incident to the structure. The other parts are modelled using the Thermoviscous Acoustics module. At the boundaries where the air makes contact with the inner wall of structure, no-slip and isothermal conditions are applied. The relative acoustic surface impedance of the whole structure is calculated as

$$z_s = \frac{\langle p \rangle}{\langle v_{\perp} \rangle} \times \frac{1}{Z_0} \quad (8)$$

where  $p$  is the total pressure,  $v_{\perp}$  is the normal velocity of air, and  $\langle \cdot \rangle$  is an operator referring to the average on the top surface of the structure. Substituting the result of (8) into (7) enables calculating the sound absorption coefficient of the structure.

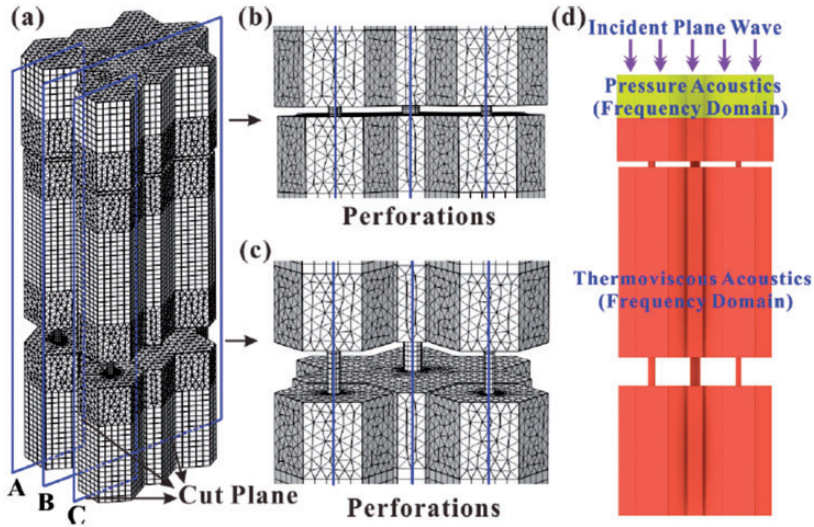


**Figure 2.** The model of numerical simulation in COMSOL Multiphysics.

Figure 3 shows the sound absorption coefficient of a micro-perforated sandwich panel with double-layer hierarchical honeycomb core in the frequency range of 50–3000 Hz. Relevant geometric parameters of the structure are given by Sample 1 of Table 1. For comparison, the results obtained for a micro-perforated sandwich panel with double-layer regular honeycomb core (Sample 2 in Table 1) are also displayed in Figure 3. For both sandwich constructions, excellent agreement is achieved between theoretical model predictions and numerical simulation results. The sound absorption coefficient continuously exceeds 0.5 from 564 Hz to 2385 Hz. In particular, beyond 1280 Hz, the sound absorption performance of the hierarchical sandwich (Sample 1) is far superior to the regular sandwich (Sample 2). In addition, the average sound absorption coefficient of the hierarchical structure is 0.474, which is 1.94 times higher than that of the regular structure. Therefore, relative to the sandwich panel with regular honeycomb core, the proposed hierarchical sandwich panel has not only enhanced mechanical properties, but also superior broadband sound absorption capability. And this is achieved with a total panel thickness of only 25 mm.

Perfect sound absorption ( $\alpha = 1$ ), meaning that the sound completely enters the interior of the structure and no reflection occurs, requires that the real part of relative acoustic surface impedance is equal to 1 and the imaginary part is equal to 0. In Figure 3, when the frequency of incident sound wave is 670 Hz and 1440 Hz, the sound absorption coefficient of the hierarchical sandwich reaches 0.970 and 0.967, respectively. Correspondingly, the real and imaginary parts of the relative acoustic surface impedance are 1.342 and  $-0.224$  at 670 Hz, and 1.417 and 0.170 at 1440 Hz, as shown in Figure 4. At other incident acoustic frequencies, the relative

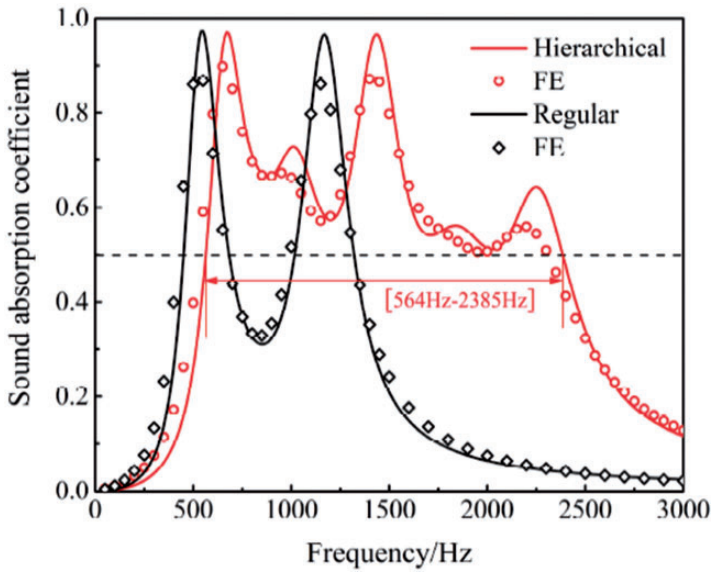


**Figure 3.** Sound absorption coefficient plotted as a function of frequency for perforated sandwich panel with double-layer hierarchical (red line and symbols) or regular (black line and symbols) honeycomb core: comparison between theoretical model predictions and FE simulation results.

**Table I.** Geometric parameters of perforated sandwich panel with double-layer hierarchical or regular honeycomb cores.

	Sample 1	Sample 2	Sample 3	Lower limit	Upper limit
$l_0/\text{mm}$	6.0	6.0	5.31	5.0	12.0
$r$	0.4	/	0.40	0.25	0.45
$l_1/\text{mm}$	2.4	/	2.12	/	/
$t_w/\text{mm}$	0.2	0.2	0.41	0.2	0.5
$d_{01}/\text{mm}$	0.7	0.7	0.64	0.2	1.0
$d_{02}/\text{mm}$	0.7	0.7	0.26	0.2	1.0
$d_{11}/\text{mm}$	0.5	/	0.64	0.2	1.0
$d_{12}/\text{mm}$	0.5	/	0.28	0.2	1.0
$d_{21}/\text{mm}$	0.4	/	0.67	0.2	1.0
$d_{22}/\text{mm}$	0.4	/	0.22	0.2	1.0
$t_1/\text{mm}$	0.4	0.4	0.64	0.2	2.0
$t_2/\text{mm}$	2.0	2.0	0.61	0.2	2.0
$h_1/\text{mm}$	13.2	13.2	17.61	$h-2t_1-t_2-h_2$	
$h_2/\text{mm}$	9.0	9.0	5.50	2.0	18.0
$h/\text{mm}$	25.0	25.0	25.0	25.0	25.0

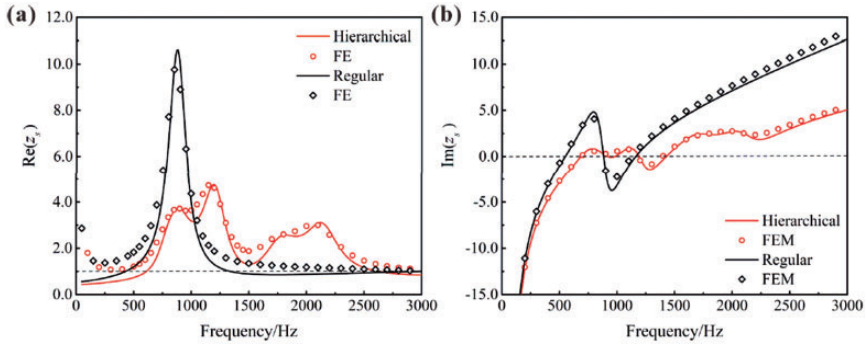


**Figure 4.** Relative acoustic surface impedance plotted as a function of frequency: (a) real part and (b) imaginary part.

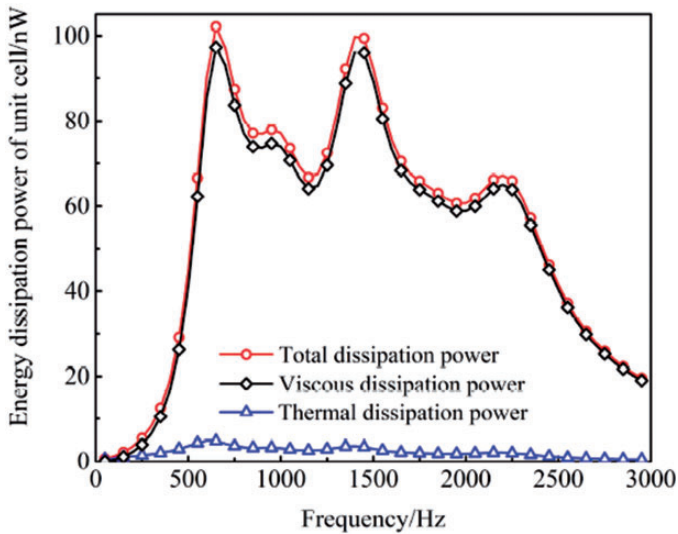


**Figure 5.** Thermal, viscous and total dissipation power of one unit cell in hierarchical sandwich.

acoustic surface impedance of the structure is far from the perfect sound absorption condition. In contrast, for the regular sandwich, only at 570 Hz and 1170 Hz, the relative acoustic surface impedance is close to the perfect sound absorption condition. At other frequencies, the acoustic surface impedance of structure is seriously mismatched with the air acoustic impedance, and most of the incident acoustic energy is reflected back with the reflected wave.

When the sound impinges on the surface of the sandwich, part of the energy is absorbed by the structure and then converted to heat via viscous and thermal dissipation of the air. Figure 5 presents the thermal, viscous and total dissipation

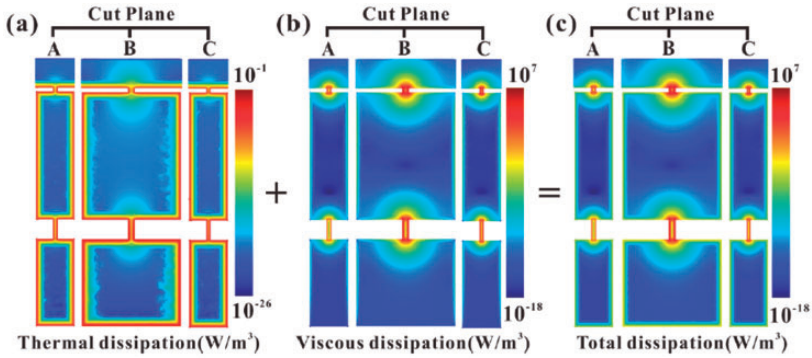


**Figure 6.** Thermal, viscous and total dissipation power at 650 Hz in three cut planes of hierarchical sandwich.

power numerically calculated for one unit cell of the hierarchical sandwich at different frequencies. The variation trend of sound absorption displayed in Figure 3 is almost the same as that of total dissipation power. Thermal dissipation is negligibly small in the whole frequency range, and most of the sound energy is dissipated within viscous boundary layers between air and solid surfaces. It is interesting to notice that, a variety of coiled structures have been proposed to lengthen the propagation path of air and hence enlarge viscous dissipation so as to achieve enhanced sound absorption performance at relatively low frequencies [29,30].

Figure 6 presents the thermal, viscous and total dissipation power at 650 Hz in the three cut planes A, B, and C of the hierarchical sandwich. When the incident frequency is close to the resonance frequency, air oscillation in the micro-perforations becomes increasingly intense. In the viscous boundary layer inside each micro-perforation and the radiation region of its inlet and outlet, a large amount of acoustic energy is constantly converted into heat. Compared with viscous dissipation, thermal dissipation mainly occurs on the solid walls of the structure and its magnitude is negligibly small. The viscosity of air in and around the micro-perforations dominates sound energy dissipation, and hence it is reasonable to only consider this factor in theoretical analysis.

### *Effect of geometric parameters on sound absorption*

The sound absorption performance of a micro-perforated hierarchical sandwich is closely related to its topological configuration. Figure 7 shows the influence of top faceplate thickness on sound absorption coefficient. The remaining geometrical parameters are the same as Sample 1 in Table 1. As the top faceplate thickness is reduced, multiple sound absorption peaks appear. For example, when the top faceplate is as thin as 0.4 mm (so as to be consistent with Figure 3), five sound absorption peaks appear at 670 Hz, 1010 Hz, 1440 Hz, 1840 Hz and 2250 Hz. As a

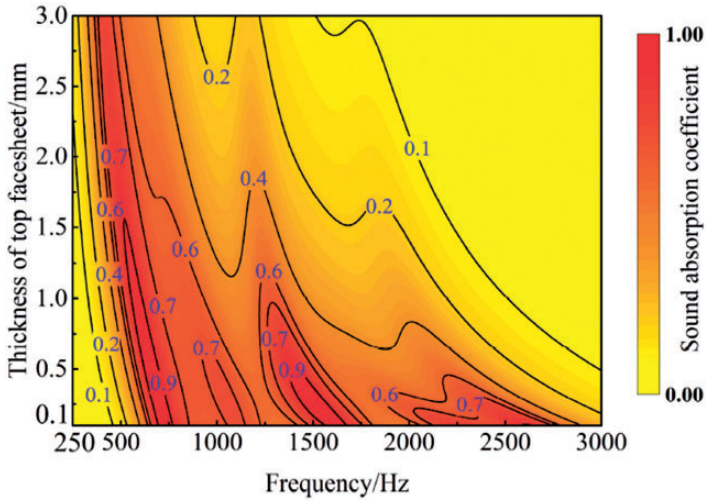


**Figure 7.** Effects of top faceplate thickness on sound absorption coefficient of micro-perforated hierarchical sandwich.

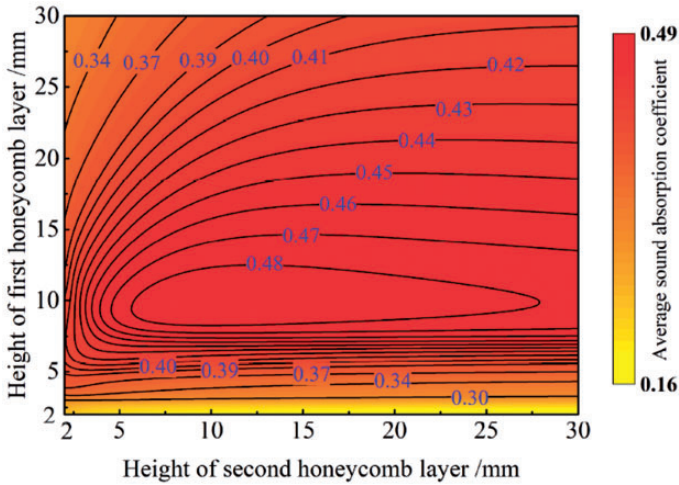


**Figure 8.** Effect of hierarchical honeycomb height on average sound absorption coefficient (between 50 and 3000 Hz).

result, the structure exhibits superior broadband sound absorption performance relative to the regular honeycomb sandwich.

Figure 8 illustrates the effect of hierarchical honeycomb height on average sound absorption coefficient from 50 Hz to 3000 Hz. Except for the thickness of

the two honeycomb layers, other parameters are the same as Sample 1 in Table 1. Sound absorption of the structure is seen to be more sensitive to the height of the first honeycomb layer. When the height of the first layer falls within the range of 7.5–12.5 mm and that of the second layer lies in the range of 5.0–27.5 mm, the structure exhibits relatively enhanced sound absorption performance.

The effects of middle faceplate thickness and its position (equivalently, height of the second honeycomb layer) on the average sound absorption coefficient (from 50 Hz to 3000 Hz) of the hierarchical sandwich are displayed in Figure 9, with its total thickness fixed at 25 mm. To this end, the height of the first honeycomb layer varies with the thickness of the middle faceplate and its position as  $h_1 = h - 2t_1 - t_2 - h_2$ , while the remaining geometrical parameters are the same as Sample 1. When the top faceplate thickness is within the range of 1.0–3.0 mm and the height of the second honeycomb layer lies in the range of 10–14 mm, the proposed structure exhibits relatively enhanced sound absorption performance.

### Optimization of sound absorption

For maximized sound absorption performance, the topological configuration of the hierarchical sandwich proposed in the present study, denoted here as  $X = [l_0, r, t_w, d_{01}, \dots, d_{22}, t_1, t_2, h_1, h_2]$ , is optimized using the simulated annealing algorithm [31,32]. In metallurgy, annealing refers to heat an alloy above its recrystallization temperature, maintain a certain period of time for grain growth, and then cool it down slowly, so as to achieve refined grains, less defects and enhanced toughness. From the point of view of statistical mechanics, the slow process of

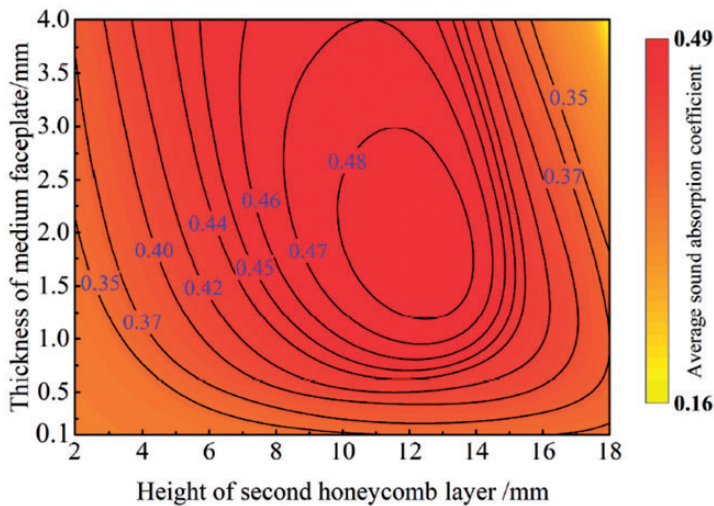


**Figure 9.** Effects of middle faceplate thickness and its position on average sound absorption coefficient (between 50 and 3000 Hz) with total thickness of the hierarchical sandwich fixed at 25 mm.

cooling allows the material to reach a temporary minimum free energy state at each temperature. When the material is completely cooled, the free energy is minimized globally. Mathematically, the method of simulated annealing describes the annealing process that enables the free energy gradually to reach the minimum. For the problem considered in the current study, the optimization target is set as: maximize the average sound absorption coefficient of the sandwich structure over a specific frequency band of interest. The optimization process is illustrated schematically in Figure 10, which may be divided into the following main steps:

1. Start the simulated annealing program. Preset the control parameters of optimization (initial annealing temperature  $T_i$ , final equilibrium temperature  $T_f$ , maximum number of iterations  $L$ , and cooling factor  $\beta$ ) and the range of

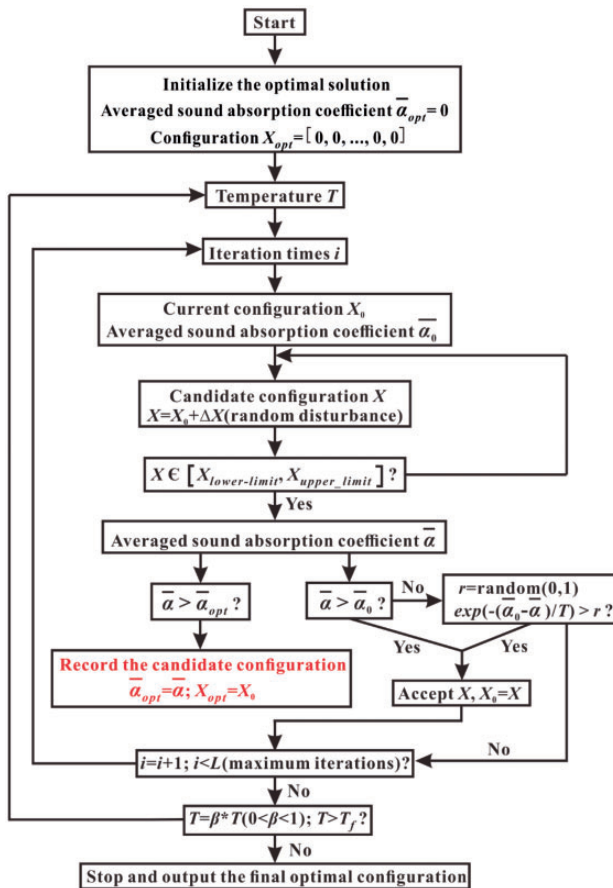


**Figure 10.** Flow chart of simulated annealing algorithm for optimized average sound absorption with hierarchical sandwich.

- structural parameters. Initialize the optimal average sound absorption coefficient and structural configuration as:  $\bar{\alpha}_{opt} = 0$  and  $X_{opt} = [0, 0, \dots, 0]$ .
2. Arbitrarily give a structural configuration  $X_0$  within the parameter range and calculate the average sound absorption coefficient  $\bar{\alpha}_0$ .
  3. Randomly generate a set of structural parameters  $X$ . If  $X$  is within the range of structural parameters, calculate the average sound absorption coefficient  $\bar{\alpha}$ . Otherwise, randomly regenerate a new set of structural parameters.
  4. If  $\bar{\alpha} > \bar{\alpha}_{opt}$ , temporarily consider  $X$  as the optimal configuration:  $\bar{\alpha}_{opt} = \bar{\alpha}$ ,  $X_{opt} = X$ .
  5. If  $\bar{\alpha} > \bar{\alpha}_0$ , accept the candidate configuration:  $\bar{\alpha}_0 = \bar{\alpha}$ ,  $X_0 = X$ , and execute the next loop. Otherwise, accept the candidate configuration with a small probability  $\exp(-(\bar{\alpha}_0 - \bar{\alpha})/T)$ . This acceptance criterion allows the algorithm to accept worse solutions with a small probability, enabling the optimization algorithm to skip the local optimal solution and approach the global optimal solution.
  6. Check whether the number of iterations  $i$  exceeds the maximum number of iterations  $L$ . If  $i > L$ , stop the current cycle and reduce the temperature  $T = \beta T$  ( $0 < \beta < 1$ ).
  7. Check whether the temperature  $T$  is lower than  $T_f$ . If  $T < T_f$ , stop the program and output the optimal configuration  $X_{opt}$ .

Figure 11 compares the sound absorption performance (from 50 Hz to 3000 Hz) of the proposed hierarchical sandwich structure before and after optimization. The control parameters of optimization are given as:  $(T_i, T_f, L, \beta) = (1000, 0.1, 300, 0.9)$ , and the upper and lower limits for each parameter are listed in Table 1. Sample 3 in

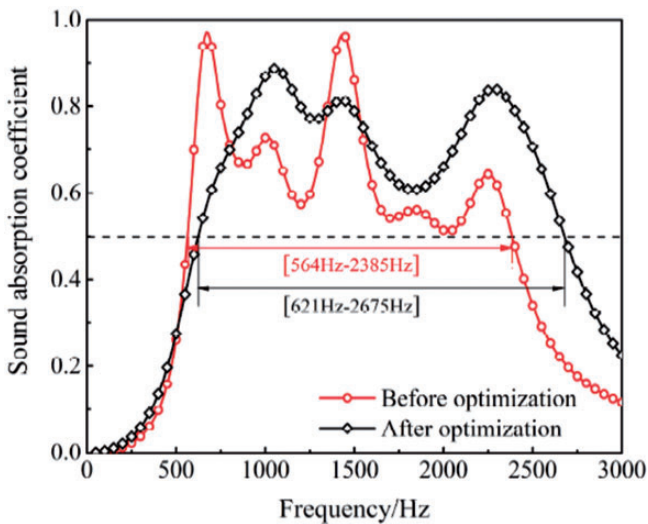


**Figure 11.** Sound absorption coefficient (before and after optimization) plotted a function of frequency for hierarchical sandwich with fixed total thickness of 25 mm.

Table 1 summarizes the geometrical parameters of the obtained optimal structure. In the range of 520 to 1530 Hz, the sound absorption performance of the sandwich before and after optimization has its own advantages, but at other frequencies, especially after 1530 Hz, the performance of the optimized structure (Sample 3) is greatly improved relative to Sample 1 before optimization. Besides, the half-absorption bandwidth is significantly widened. From 621 to 2675 Hz, the sound absorption coefficient of the optimized structure continuously exceeds 0.5. Further, while the average absorption coefficient of the original structure from 50 to 3000 Hz is only 0.474, that of the optimized structure is 0.571, an increase of 20.46%.

## Conclusions

A combined theoretical and numerical study has been carried out to evaluate the sound absorption performance of a novel ultralight micro-perforated sandwich panel with double-layer hierarchical hexagonal honeycomb core, which also possesses excellent load-bearing capability. Theoretical model predictions match well with full finite element simulation results. For comparison, a micro-perforated sandwich panel with regular honeycomb core is also investigated. Systematic parametric study is implemented to investigate the influence of key topological parameters on sound absorption. To obtain optimal sandwich configuration for sound absorption, the method of simulated annealing is employed.

It is demonstrated that the micro-perforations with different sub-millimeter diameters on selected faceplates and the air cavities divided by the hierarchical honeycomb enable multiple absorption peaks, leading to significantly widened half-absorption bandwidth relative to the regular honeycomb sandwich. Numerical simulations considering the thermo-viscous effects of air reveal that when the frequency of incident sound reaches the resonance frequency, air oscillations in micro-perforations intensify, and the energy of sound is dissipated mainly due to the viscosity of air. Both the faceplate thickness and the height of the first layer honeycomb have important influence on sound absorption. The proposed hierarchical honeycomb sandwich exhibits superior sound absorption in comparison with the regular honeycomb sandwich, in addition to significantly enhanced load-bearing capability. This ultralight sandwich configuration has great potential in aeronautic and aerospace engineering where excellent mechanical and acoustic properties as well as light weight and small volume are simultaneously required.

## Authors' Note

Wei He and Xiangjun Peng are no long affiliated to State Key Laboratory of Mechanics and Control of Mechanical Structures, Nanjing University of Aeronautics and Astronautics, Nanjing, P.R. China. Tian J Lu is no longer affiliated to MOE Key Laboratory for Multifunctional Materials and Structures, Xi'an Jiaotong University, Xi'an, P. R. China.

## Acknowledgements

This work was supported by the National Natural Science Foundation of China (52075416, 11772248, 11761131003 and U1737107) and the German Research Foundation (ZH 15/32–1).

## Declaration of Conflicting Interests

The author(s) declared no potential conflicts of interest with respect to the research, authorship, and/or publication of this article.

## Funding

The author(s) received no financial support for the research, authorship, and/or publication of this article.

## ORCID iD

Fengxian Xin  <https://orcid.org/0000-0001-8855-5366>

## References

1. Baer E, Hiltner A and Keith HD. Hierarchical structure in polymeric materials. *Science* 1987; 235: 1015–1022.
2. Chen Q and Pugno NM. Bio-mimetic mechanisms of natural hierarchical materials: a review. *J Mech Behav Biomed Mater* 2013; 19: 3–33.
3. Espinosa HD, Juster AL, Latourte FJ, et al. Tablet-level origin of toughening in abalone shells and translation to synthetic composite materials. *Nat Commun* 2011; 2: 173.
4. Song J, Fan C, Ma H, et al. Crack deflection occurs by constrained microcracking in nacre. *Acta Mech Sin* 2018; 34: 143–150.
5. Ajdari A, Jahromi BH, Papadopoulos J, et al. Hierarchical honeycombs with tailorable properties. *Int J Solids Struct* 2012; 49: 1413–1419.
6. Mousanezhad D, Babaee S, Ebrahimi H, et al. Hierarchical honeycomb auxetic metamaterials. *Sci Rep* 2015; 5: 18306.
7. Haghpanah B, Oftadeh R, Papadopoulos J, et al. Self-similar hierarchical honeycombs. *Proc R Soc A* 2013; 469: 20130022.
8. Haghpanah B, Papadopoulos J and Vaziri A. Plastic collapse of lattice structures under a general stress state. *Mech Mater* 2014; 68: 267–274.
9. Sun GY, Jiang H, Fang JG, et al. Crashworthiness of vertex based hierarchical honeycombs in out-of-plane impact. *Mater Des* 2016; 110: 705–719.
10. Ryvkin M and Shraga R. Fracture toughness of hierarchical self-similar honeycombs. *Int J Solids Struct* 2018; 152–153: 151–160.
11. Maa DY. Theory and design of microperforated-panel sound-absorbing. *Sci Sin* 1975; 18: 55–71.
12. Maa DY. Potential of microperforated panel absorber. *J Acous Soc Am* 1998; 104: 2861–2866.
13. Ren SW, Van Belle L, Claeys C, et al. Improvement of the sound absorption of flexible micro-perforated panels by local resonances. *Mech Syst Signal Proc* 2019; 117: 138–156.
14. Lee DH and Kwon YP. Estimation of the absorption performance of multiple layer perforated panel systems by transfer matrix method. *J. Sound Vib* 2004; 278: 847–860.

15. Ruiz H, Cobo P and Jacobsen F. Optimization of multiple-layer microperforated panels by simulated annealing. *Appl Acoust* 2011; 72: 772–776.
16. Yang XC, Bai PF, Shen XM, et al. Optimal design and experimental validation of sound absorbing multilayer microperforated panel with constraint conditions. *Appl Acoust* 2019; 146: 334–344.
17. Zhou H, Wang X, Wu H, et al. The vibroacoustic response and sound absorption performance of multilayer, microperforated rib-stiffened plates. *Acta Mech Sin* 2017; 33: 926–941.
18. Wang C and Huang L. On the acoustic properties of parallel arrangement of multiple micro-perforated panel absorbers with different cavity depths. *J Acous Soc Am* 2011; 130: 208–218.
19. Wang C, Cheng L, Pan J, et al. Sound absorption of a micro-perforated panel backed by an irregular-shaped cavity. *J Acoust Soc Am* 2010; 127: 238–246.
20. Min HQ and Guo WC. Sound absorbers with a micro-perforated panel backed by an array of parallel-arranged sub-cavities at different depths. *Appl Acoust* 2019; 149: 123–128.
21. Mosa AI, Putra A, Ramlan R, et al. Theoretical model of absorption coefficient of an inhomogeneous MPP absorber with multi-cavity depths. *Appl Acoust* 2019; 146: 409–419.
22. Kimihiro S and Masayuki M. Application of microperforated panel absorbers to room interior surfaces. *Int J Acoust Vib* 2008; 13: 120–124.
23. Kimihiro S, Ipei Y, Motoki Y, et al. Sound absorption characteristics of a honeycomb-backed microperforated panel absorber revised theory and experimental validation. *Noise Control Eng. J* 2010; 58: 157–162.
24. Toyoda M, Sakagami K, Takahashi D, et al. Effect of a honeycomb on the sound absorption characteristics of panel-type absorbers. *Appl Acoust* 2011; 72: 943–948.
25. Ingard U. On the theory and design of acoustic resonators. *J Acous Soc Am* 1953; 25: 1037–1061.
26. Omrani A and Tawfiq I. Vibro-acoustic analysis of micro-perforated sandwich structure used in space craft industry. *Mech Syst Signal Proc* 2011; 25: 657–666.
27. Tang YF, Ren SW, Meng H, et al. Hybrid acoustic metamaterial as super absorber for broadband low-frequency sound. *Sci Rep* 2017; 7: 44972.
28. Tang YF, He W, Xin FX, et al. Nonlinear sound absorption of ultralight hybrid-cored sandwich panels. *Mech Syst Signal Proc* 2020; 135: 106428.
29. Li Y and Assouar BM. Acoustic metasurface-based perfect absorber with deep subwavelength thickness. *Appl Phys Lett* 2016; 108: 063502.
30. Wu F, Xiao Y, Yu DL, et al. Low-frequency sound absorption of hybrid absorber based on micro-perforated panel and coiled-up channels. *Appl Phys Lett* 2019; 114: 151901.
31. Metropolis N, Rosenbluth AW, Rosenbluth MN, et al. Equation of state calculations by fast computing machines. *J Chem Phys* 1953; 21: 1087–1092.
32. Kirkpatrick S, Gelatt JCD and Vecchi MP. Optimization by simulated annealing. *Science* 1983; 220: 671–680.